Scientia Iranica F (2019) 26(6), 3889–3895

Sharif University of Technology
Scientia Iranica
Transactions F: Nanotechnology
http://scientiairanica.sharif.edu

Application of microwave-assisted synthesized leaf-like ZnO nanosheets as the ethanol sensor

Gh. Kiani*, **A. Nourizad**, **and R. Nosrati**

School of Engineering, Emerging Technologies, University of Tabriz, Tabriz, 5166616471, Iran.

Received 26 August 2018; received in revised form 22 February 2019; accepted 13 May 2019

KEYWORDS
Ethanol sensing;
Gas sensor;
Leaf-like ZnO;
Mesoporous;
Nanosheets;
Microwave.

Abstract. In this study, leaf-like zinc oxide (ZnO) nanosheets were successfully synthesized by the microwave-assisted method through an easy, low-cost solvothermal process with annealing at 500°C. Characterization of the synthesized material revealed the mesoporous single-crystal leaf-like ZnO nanosheets with hexagonal wurtzite structure. Mesoporous and single-crystal structure of gas sensor could provide high surface area, which led to the diffusion of gas molecules and improvement of gas sensitivity. Consequently, the gas-sensing function of the leaf-like ZnO nanosheets was tested for different types of Volatile Organic Compounds (VOCs). Sensitivity, stability, response, and recovery time of leaf-like ZnO nanosheets sensor for ethanol vapor were the best at 255°C. According to results, leaf-like ZnO nanosheets are a selective and sensitive sensor for ethanol vapor.

1. Introduction

During the last two decades, the environment has been contaminated considerably by cars, factories, and other diverse, harmful pollutants. The major part of the so-called pollutions is a kind of hydrocarbon compounds, such as ethanol, methanol, acetone, benzene, hexane, toluene, and so on, classified as Volatile Organic Compounds (VOCs) having boiling points below 200°C. They are used in most parts of chemical industries as solvents. They can be sick agents causing allergies, asthma, cancer, and emphysema in human being. Therefore, many studies have focused on the development of the VOCs sensing materials, including organic and inorganic semiconductors as well as their hybrids [1-3]. Metal Oxide Semiconductors (MOSs) as inorganic materials, such as SnO_2, ZnO, TiO_2, Fe_2O_3, In_2O_3, and so on, are potential gas-sensing materials [4]. Singh et al. [5] made a highly sensitive ethanol sensor based on TiO_2 nanoparticles with the sensitivity of ~ 0.052 mAM^{-1}cm^{-2}. Yang et al. [6] prepared a highly efficient ethanol gas sensor based on hierarchical SnO_2/Zn_2SnO_4 porous spheres and reached a response of 30.5 toward 100 ppm ethanol in the optimum operating temperature of 250°C. Li et al. [7] decorated the Zn_2SnO_4 nanoparticles on reduced graphene oxide and investigated its performance for ethanol sensing. The response of the fabricated sensor to 100 ppm ethanol at the optimal operating temperature of 275°C was as high as 38.

Zinc oxide is an *n*-type wide-bandgap semiconductor in the II-VI semiconductor group. It has extensively been utilized in the fields of sensors and photocatalytic activities. In order to enhance ZnO sensing property, nanostructuring and nano miniaturizing is one of the popular strategies. It has been revealed that the gas sensing property increases rapidly when the particle size becomes comparable to or smaller than the Debye length. However, due to high-temperature performance, usually above 200°C, of nano-size ZnO material coated as a thin film on substrates in sensing

*. *Corresponding author. Tel.: +98 4133393853;*
Fax: +98 4133294626
E-mail addresses: g.kiani@tabrizu.ac.ir (Gh. Kiani);
a.norizad1364@gmail.com (A. Nourizad);
ra.nosrati@gmail.com (R. Nosrati)

doi: 10.24200/sci.2019.51664.2300

applications, the nano effect of ZnO is influenced by its unrestrained agglomeration to a certain extent, because the van der Waals attraction is inverse to the size of the particle. Hence, homogeneous dispersion of nanoparticles is important and can be achieved through a liquid medium by stirring [8].

Different morphologies of ZnO nanostructure have been successfully synthesized and fabricated, including nanorods [9-12], nanowires [13], floccule-like [14], tetrapod-like [15,16], nanotubes [17], flower-like [18,19], spindle-like [20], nanosheets [21,22], and nanoparticles [23,24], in order to exploit the miniature-size, highly dense surface sites, and increasing surface-to-volume ratios for enhancing the performance of the sensors.

Different types of synthesis have been applied to preparing ZnO, such as precipitation method, sol-gel, hydrothermal, and so on [25-28]. In the present work, we report hierarchically porous single-crystal leaf-like ZnO nanosheets, which were successfully synthesized through an easy, economical, microwave-assisted solvothermal process [29,30] pursued by annealing of the pre-synthesized material at 500°C for 3 hours in the air atmosphere.

The sensors made of zinc oxide respond excellently to ethanol vapor. Characteristics such as ultrahigh sensitivity, rapid response and recovery time, best selectivity, and long-term stability are enhanced. The surface atomic structure and morphology of the sensor were analyzed through SEM, EDS, and XRD in this study.

2. Materials and methods

2.1. Materials

Zinc nitrate, ethanol (%99.5), methanol, ammonia, benzene, and toluene were purchased from Merck chemicals, Germany. Acetone and formaldehyde were obtained from Sigma Aldrich and Kilco, England, respectively. Deionized water was used in all experiments.

2.2. Preparation of leaf-like ZnO nanosheets

In a typical experiment, 4 g zinc nitrate was dissolved in 80 mm ethanol. After stirring vigorously for 30 min, the homogeneous solution was transferred into a Teflon-liner autoclave reactor and then, put into a microwave system. The reaction was conducted at 900 W for 2 hours.

After cooling to room temperature, the products were washed and centrifuged with deionized water and absolute ethanol several times. Then, the as-prepared products were collected and dried at 80°C for 10 hours. In order to obtain the final leaf-like ZnO nanosheets, the precipitate was calcinated at 500°C for 3 hours by means of electrical furnace [31].

2.3. Preparation of the gas sensor

In order to test the gas response, interdigitated electrodes with 150 μm gap distance from each other on the one side and a heater on the other side were printed on substrate as shown in Figure 1. The leaf-like ZnO nanosheets powder was dispersed in deionized water and ultrasonicated for 30 min to obtain a homogenous solution. Then, the solution was spread over interdigitated electrodes by using a micropipette and spin coater spinning with 900 rpm for 4 min. The coated substrates were heated to remove the solvent at 50°C for 45 min.

2.4. Measurement of gas sensor properties

In order to evaluate the gas sensing properties of the pre-fabricated sensor, its electrical resistance was measured indirectly by using the circuit presented in Figure 2. In this circuit, R_h as a heater resistance value is used to heat the sensor to the desired temperature and V_h is the applied voltage across the heater element. R_s represents the variable resistance value of the sensor and V_s is the voltage over the sensors. R_L as sample resistance is used in order to measure the flowing current through the sensor and V_L is the corresponding

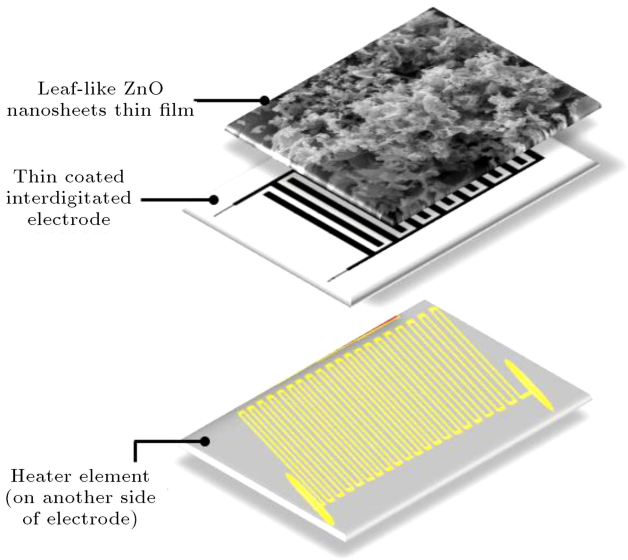

Figure 1. Structure of the sensor.

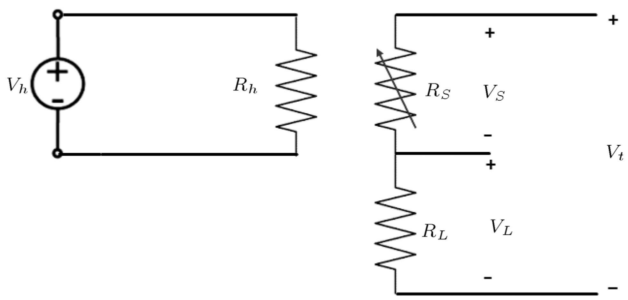

Figure 2. Electric circuit for gas sensing measurement.

voltage over R_L. The sensor current is calculated at the left part of Eq. (1). V_t is total voltage to bias the circuit of serial sensor resistor (R_s) and sampled resistor (R_L), and finally, R_s is the resistance of a sensor, which can be determined indirectly by Eq. (1).

$$\begin{aligned} I_L = V_L/R_L \\ \Longrightarrow R_S = V_S/I_L = ((V_t - V_l) * R_L)/V_L \\ V_S = V_t - V_L. \end{aligned} \tag{1}$$

In order to evaluate gas sensing property of the as-prepared leaf-like (ZnO) nanosheets sensor, the home-made gas tester was designed and fabricated with a volume of 16 liters. In order to remove any pollutions, nitrogen (N_2) gas was inserted in the as-neutral gas and taken out by another tap. Then, fresh air provided by the electric air pump was inserted in the tester through homemade humidity maker chamber. The relative humidity was stabled by humidity sensors at 40 percent before and during the test. The temperature sensor was used to monitor the temperature inside the tester. Two fans were installed on the wall of the tester to homogenize the inside of the chamber. After reaching stability of the sensor resistance, the testing gas was injected into the tester as a liquid by Eq. (2):

$$\begin{aligned} n = m_g/V_{\text{chamber}} \\ \Longrightarrow V_g = nV_{\text{chamber}}/D_g \\ V_g = m_g/D_g, \end{aligned} \tag{2}$$

where n is gas concentration (ppm), m_g is liquid gas mass (milligram), V_{chamber} is gas volume (16 L), and D_g is gas density. After a definite time, the gas was evacuated through the outlet lid, which was located above the tester as shown in Figure 3.

2.5. Characterization

Microwave system and hydrothermal reactor were used for synthesis. For the calcination of leaf-like ZnO nanosheets, an electrical furnace shimaz20 was used. X-Ray Diffraction (XRD) patterns and SEM micrographs of samples were obtained by D5000 X-ray diffractometer and MIRA3 TESCAN Scanning Electron Microscope, respectively.

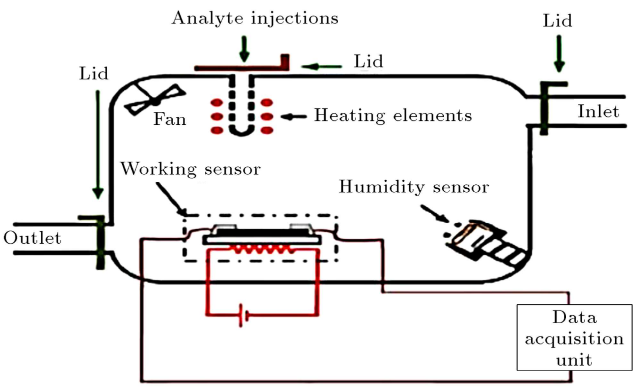

Figure 3. Schematic diagram of the gas tester set-up.

3. Results and discussion

3.1. X-ray diffraction patterns

To investigate the crystalline structure of leaf-like ZnO nanosheets, X-Ray Diffraction (XRD) analysis was performed. Figure 4 shows the XRD patterns of the as-prepared leaf-like ZnO nanosheets. All peaks were well related to tetragonal ZnO (JCPDS 36-1451). No other crystal phase was detected, indicating the high purity of the final product.

In the annealing process, the crystalline nature of the zinc oxide was improved at higher annealing temperatures. It might be due to the annealing temperature, providing enough energy for orientation toward proper equilibrium sites, resulting in the improvement of crystallinity and degree of orientation of the zinc oxide [32]. The crystallite size was calculated using the Scherrer equation ($D = 0.89\lambda/\beta\cos(\theta)$), where D is the average crystal size in nm, λ is the X-ray wavelength (CuK_α : 0.15406 nm), β is the Full Width at Half-Maximum (FWHM) of the peak, and θ is the corresponding Bragg diffraction angle. The average crystallite size of the leaf-like ZnO nanosheets, which was calculated by the Scherer formula at the FWHM (101) and $2\theta = 36.45°$, was approximately 19.53 nm.

3.2. Morphological studies

The morphology of the as-synthesized leaf-like ZnO nanosheets was characterized via SEM as shown in Figure 5. Figure 5(a) illustrates a sample image of the as-prepared ZnO nanosheets that made up irregular patterns of leaf-like nanosheets with 5-10 μm diameter and 10-40 nm edge thicknesses. The magnified image (Figure 5(c)) exhibits that the ZnO nanosheets have rough surfaces and dense pores. Figure 5(b) shows the image of the structure with random pores spread on the ZnO nanosheets, which may result in higher surface area, better gas diffusion, and more active sites. Especially, the figure shows that the total structure of as-prepared ZnO is leaf-like. Also, annealing increases the uniformity of leaf-like nanostructures of ZnO as confirmed by the SEM images.

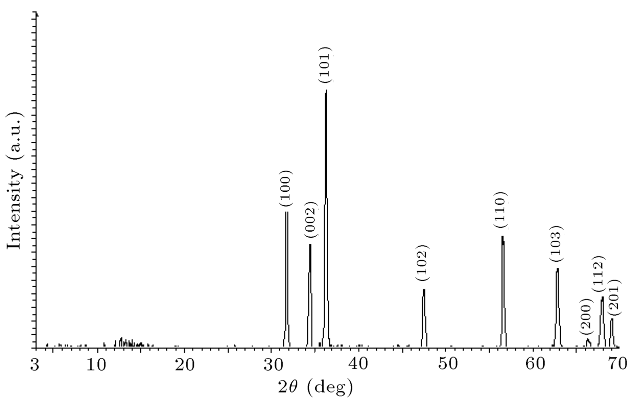

Figure 4. XRD pattern of leaf-like 2D ZnO nanosheets.

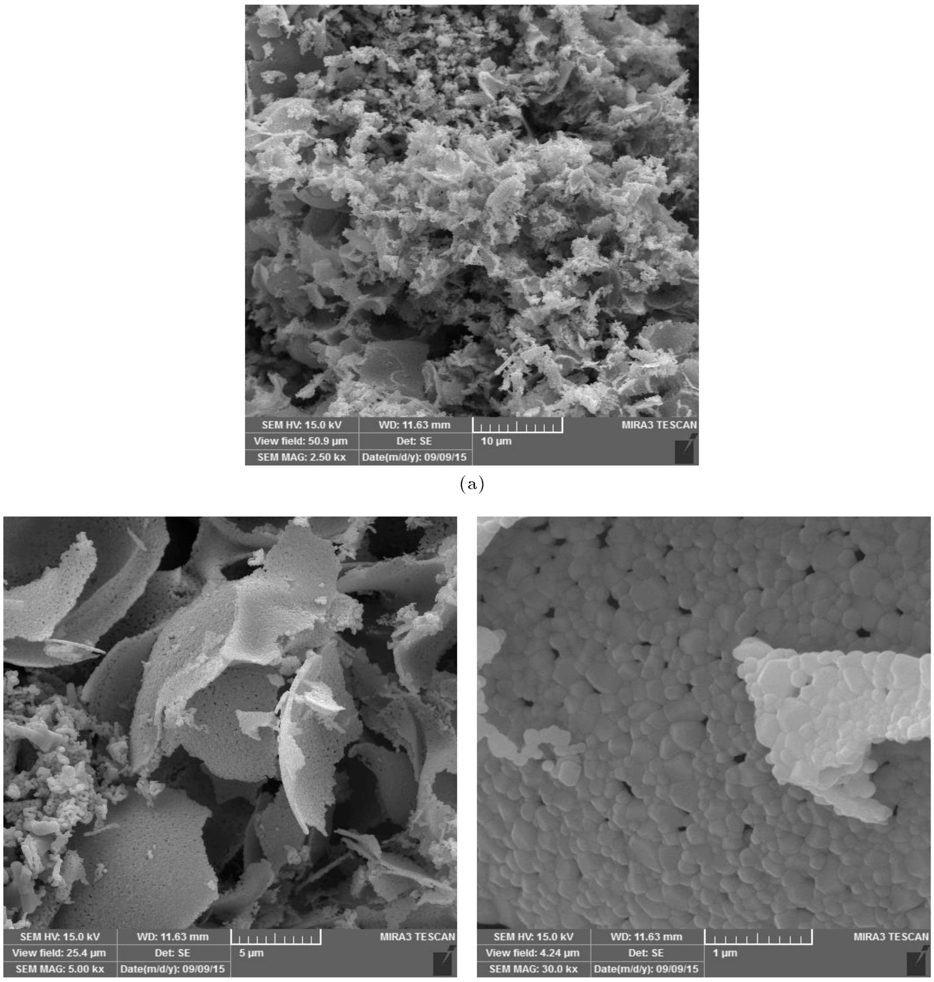

Figure 5. SEM images of leaf-like ZnO nanosheets in (a) low, (b) medium, and (c) high magnifications.

3.3. EDX analysis

As presented in Figure 6, it can clearly be deduced from the analysis of the Energy-Dispersive X-ray spectroscopy (EDX) that zinc and oxygen elements were present in the synthesized material with no other element. Therefore, the synthesized product was approximately pure.

3.4. Gas sensing properties

Figure 7 shows the response of the leaf-like ZnO nanosheets sensor to 100 ppm ethanol vapor at different working temperatures to determine the optimal operating temperature. The result indicates that it is about 255°C. Sensitivity of the sensor is calculated by using the equation:

$$S = R_a/R_g,$$

where R_g is the resistance of sensor in the presence of gas and R_a is the resistance of sensor in the air. At the optimal working temperature, the sensor has the highest response of 51 to 100 ppm ethanol vapor. According to the literature, the responses of different ZnO nanostructures including flower-like ZnO, Cr-doped ZnO, and 3-D hierarchical porous ZnO are 30.4, 45, and 36.6, respectively. The mentioned

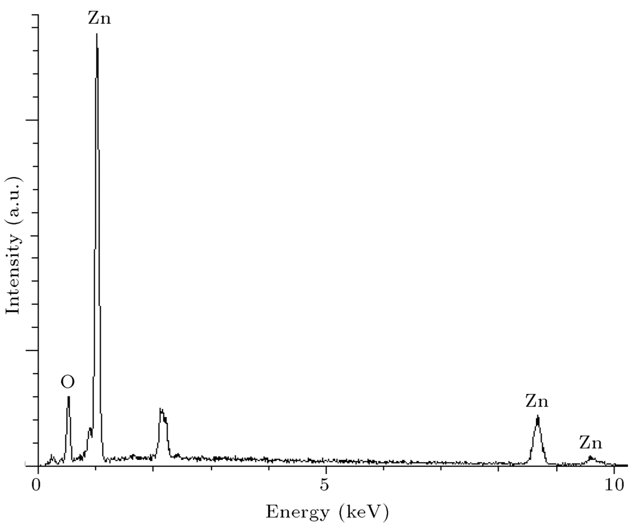

Figure 6. EDS analysis of the leaf-like ZnO nanosheets.

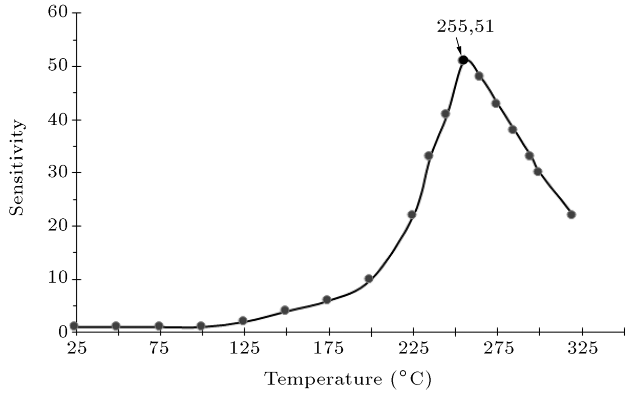

Figure 7. Response of the leaf-like ZnO nanosheets probed at different temperatures to 100 ppm ethanol vapor (in order to investigate the optimal temperature).

sensors act in relatively high temperatures and the ethanol gas concentrations are 400, 400, and 50 ppm, respectively [33].

All of the tests were performed at 255°C. It is clear from Figure 8(a) that the sensing range of the sensor is vast, approximately linear, especially for concentrations more than 100 ppm. Sensor response does not saturate even to higher ethanol concentrations. It can be due to the existence of more active sites. The sensor responds to 100 ppm different organic and inorganic gases including methanol, ethanol, acetone, ammonia, formaldehyde, benzene, and toluene. Figure 8(b) reveals that selectivity for ethanol vapor is high and other VOCs and inorganic gases are suppressed. In other words, the leaf-like ZnO nanosheets sensor has a low cross-sensing property. Stronger reaction between leaf-like ZnO nanosheets and ethanol than between other gases may be the cause of this phenomenon [34]. It can be concluded from Figure 8(c) that repeatability of the sensor is good. Its response and recovery time are approximately 220 and 145 seconds, respectively. In order to investigate stability of the sensor, the response of the sensor to 100 ppm ethanol vapor was checked every 10 days for three months. The result showed good stability as illustrated in Figure 9.

3.5. Gas sensing mechanism

Sensing mechanism can be described as follows: on the surface of the sensor, atmospheric oxygen molecules were decomposed by high temperature to oxygen ions such as O_2^-, O^-, and O^{2-}, as represented in Eqs. (3)-(7). Negative oxygen ion species obtained electrons from ZnO and made the depletion layer [35]. When the sensor was exposed to ethanol as a reducing gas, the adsorbed oxygen ions reacted with ethanol vapor and released the adsorbed electrons. Subsequently, resistance of the sensor significantly decreased (Eq. (7)).

$$O_2(\text{gas}) \xleftrightarrow{255^\circ C} O_2(\text{ads}), \tag{3}$$

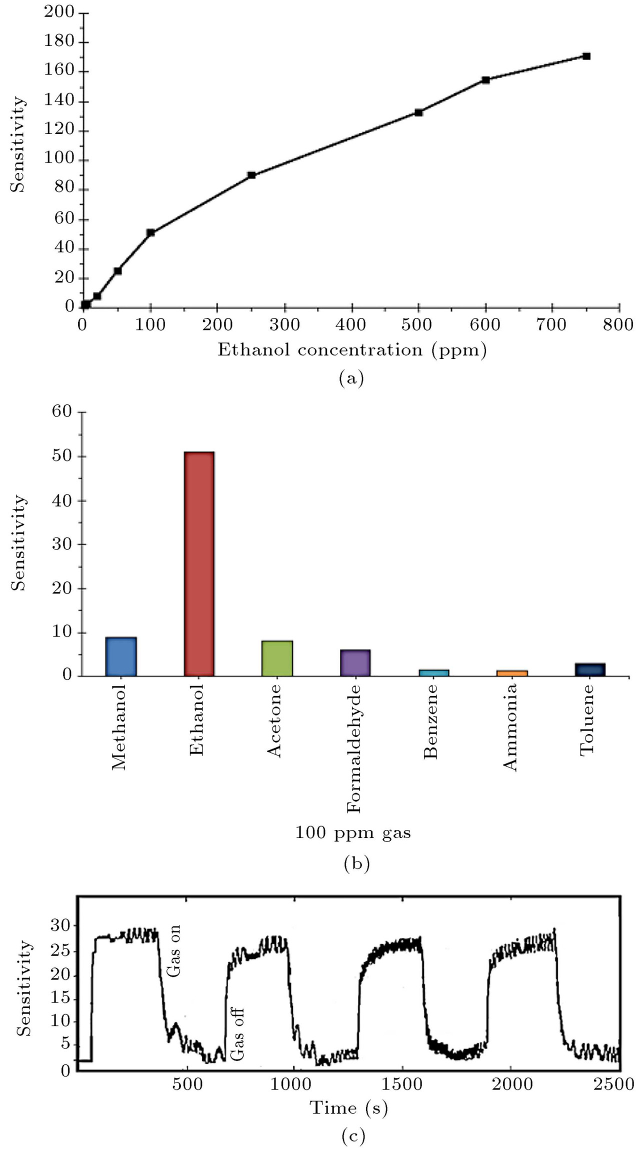

Figure 8. (a) Response of the sensor to different ethanol concentrations (linearity). (b) Selectivity and (c) repeatability investigation of the sensor for different types of gases.

$$O_2(\text{ads}) + e^- \xleftrightarrow{255^\circ C} O_2^-(\text{ads}), \tag{4}$$

$$O_2^-(\text{ads}) + e^- \xleftrightarrow{255^\circ C} 2O^-(\text{ads}), \tag{5}$$

$$O_2(\text{ads}) + 2e^- \xleftrightarrow{255^\circ C} 2O^{2-}(\text{ads}), \tag{6}$$

$$C_2H_5OH + O_2^- \xleftrightarrow{255^\circ C} C_2H_3OH + H_2O + e^-. \tag{7}$$

Eqs. (3)-(7) con note that performance of the sensor strongly depends on diverse factors such as interaction of target gas and oxygen ions, density of the active sites, porosity, and surface to volume ratio, which were met in the presented sensor, leading to improved sensor parameters.

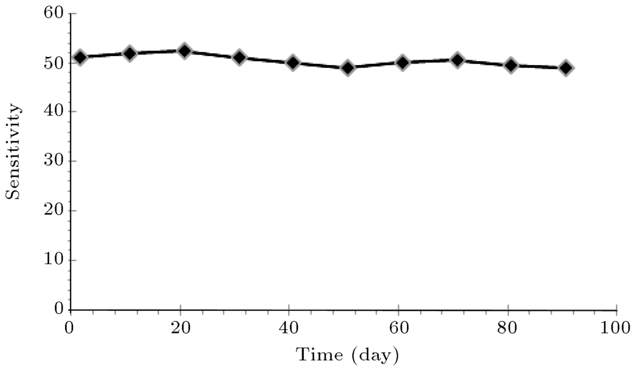

Figure 9. Stability investigation of the sensor.

The enhanced gas sensing property of leaf-like ZnO nanosheets can be due to the good permeability of leaf-like morphology of ZnO, resulting in good gas diffusion and mass transfer on the surface or in the inner region, hence the increase in adsorption and the amount of ionization oxygen on the ZnO nanosheets [36].

4. Conclusions

Low-cost, easily synthesized leaf-like ZnO nanosheets were successfully prepared by microwave-assisted solvothermal method. The porous surface of ZnO nanosheets was rough and uniform as confirmed by SEM images and EDS analyses. The improved gas sensitivity at the low temperature of 255°C for ethanol vapor might be attributed to the effective dense pores and architecture of ZnO nanosheets. Sensitivity to 100 ppm ethanol vapor was 51 and selectivity investigation showed the best result for ethanol among different types of gases. The response and recovery times were improved.

Acknowledgments

Financial support of this research by the University of Tabriz is gratefully acknowledged.

References

1. Wang, X., Hou, S., Goktas, H., et al. "Small-area, resistive volatile organic compound (VOC) sensors using metal-polymer hybrid film based on oxidative chemical vapor deposition (oCVD)", *ACS Applied Materials & Interfaces*, **7**(30), pp. 16213-16222 (2015).
2. Righettoni, M., Amann, A., and Pratsinis, S.E. "Breath analysis by nanostructured metal oxides as chemo-resistive gas sensors", *Materials Today*, **18**(3), pp. 163-171 (2015).
3. Kim, H.-J. and Lee, J.-H. "Highly sensitive and selective gas sensors using p-type oxide semiconductors: Overview", *Sensors and Actuators B: Chemical*, **192**, pp. 607-627 (2014).
4. Wang, L., Gao, J., Wu, B., et al. "Designed synthesis of In_2O_3 Beads@ TiO_2-In_2O_3 composite nanofibers for high performance NO_2 sensor at room temperature", *ACS Applied Materials & Interfaces*, **7**(49), pp. 27152-27159 (2015).
5. Singh, P., Mabdullah, M., Sagadevan, S., et al. "Highly sensitive ethanol sensor based on TiO_2 nanoparticles and its photocatalyst activity", *Optik*, **182**, pp. 512-518 (2019).
6. Yang, X., Li, H., Li, T., et al. "Highly efficient ethanol gas sensor based on hierarchical SnO_2/Zn_2SnO_4 porous spheres", *Sensors and Actuators B: Chemical*, **282**, pp. 339-346 (2019).
7. Li, Y., Luo, N., Sun, G., et al. "In situ decoration of Zn_2SnO_4 nanoparticles on reduced graphene oxide for high performance ethanol sensor", *Ceramics International*, **44**(6), pp. 6836-6842 (2018).
8. Tamvakos, A., Calestani, D., Tamvakos, D., et al. "Effect of grain-size on the ethanol vapor sensing properties of room-temperature sputtered ZnO thin films", *Microchimica Acta*, **182**(11-12), pp. 1991-1999 (2015).
9. Shin, D.H., Lee, J.S., Jun, J., et al. "Detection of hazardous gas using multidimensional porous iron oxide nanorods-decorated carbon nanoparticles", *ACS Applied Materials & Interfaces*, **7**(3), pp. 1746-1751 (2015).
10. Zhao, J., Zou, X.X., Zhou, L.J., et al. "Precursor-mediated synthesis and sensing properties of wurtzite ZnO microspheres composed of radially aligned porous nanorods", *Dalton Transactions*, **42**(40), pp. 14357-14360 (2013).
11. He, J.-Q., Yin, J., Liu, D., et al. "Enhanced acetone gas-sensing performance of La_2O_3-doped flowerlike ZnO structure composed of nanorods", *Sensors and Actuators B: Chemical*, **182**, pp. 170-175 (2013).
12. Juwana, W.E., Prabandono, B., and Purwanto, A. "Characteristics of zinc oxide nanorods synthesized by low power DC thermal plasma", *Scientia Iranica, Transactions F, Nanotechnology*, **20**(6), p. 2348 (2013).
13. Woo, H.-S., Kwak, C.H., Chung, J.H., et al. "Highly selective and sensitive xylene sensors using Ni-doped branched ZnO nanowire networks", *Sensors and Actuators B: Chemical*, **216**, pp. 358-366 (2015).
14. Ho, Y.-H., Huang, W.S., Chang, H.C., et al. "Ultraviolet-enhanced room-temperature gas sensing by using flocculе-like zinc oxide nanostructures", *Applied Physics Letters*, **106**(18), p. 183103 (2015).
15. Thepnurat, M., Chairuangsri, T., Hongsith, N., et al. "Realization of interlinked ZnO tetrapod networks for UV sensor and room-temperature gas sensor", *ACS Applied Materials & Interfaces*, **7**(43), pp. 24177-24184 (2015).
16. Mishra, Y.K., Modi, G., Cretu, V., et al. "Direct growth of freestanding ZnO tetrapod networks for multifunctional applications in photocatalysis, UV pho-

todetection, and gas sensing", *ACS Applied Materials & Interfaces*, **7**(26), pp. 14303-14316 (2015).

17. Wang, P.-P., Qi, Q., Zou, X.X., et al. "A precursor route to porous ZnO nanotubes with superior gas sensing properties", *RSC Advances*, **3**(46), pp. 23980-23983 (2013).
18. Lin, Y., Wei, W., Wang, Y., et al. "Highly stabilized and rapid sensing acetone sensor based on Au nanoparticle-decorated flower-like ZnO microstructures", *Journal of Alloys and Compounds*, **650**, pp. 37-44 (2015).
19. Bai, S., Guo, T., Li, D.Q., et al. "Intrinsic sensing properties of the flower-like ZnO nanostructures", *Sensors and Actuators B: Chemical*, **182**, pp. 747-754 (2013).
20. Chen, X., Jing, X.Y., Wang, J., et al. "Fabrication of spindle-like ZnO architectures for highly sensitive gas sensors", *Superlattices and Microstructures*, **63**, pp. 204-214 (2013).
21. Meng, F., Hou, N., Ge, S., et al. "Flower-like hierarchical structures consisting of porous single-crystalline ZnO nanosheets and their gas sensing properties to volatile organic compounds (VOCs)", *Journal of Alloys and Compounds*, **626**, pp. 124-130 (2015).
22. Yuliarto, B., Julia, S., Iqbal, M., et al. "The effect of tin addition to ZnO nanosheet thin films for ethanol and isopropyl alcohol sensor applications", *Journal of Engineering and Technological Sciences*, **47**(1), pp. 76-91 (2015).
23. Olad, A., Asadi, N., Mohammadi Aref, S., et al. "The use of adsorption method to preparation of polyaniline/ZnO nanocomposite varistor", *Journal of Materials Science: Materials in Electronics*, **29**, pp. 9692-9699 (2018).
24. Olad, A., and Nosrati, R. "Use of response surface methodology for optimization of the photocatalytic degradation of ampicillin by ZnO/polyaniline nanocomposite", *Research on Chemical Intermediates*, **41**(3), pp. 1351-1363 (2015).
25. Chithra, M.J., Pushpanathan, K., and Loganathan, M. "Structural and optical properties of Co-doped ZnO nanoparticles synthesized by precipitation method", *Materials and Manufacturing Processes*, **29**(7), pp. 771-779 (2014).
26. He, H.-Y. and Shen, Q. "Template effects of microstructure and property of sol-gel-deposited ZnO: Al: Mo films", *Materials and Manufacturing Processes*, **29**(10), pp. 1157-1161 (2014).
27. Mughal, A.J., Carberry, B., Speck, J.S., et al. "Structural and optical properties of group III doped hydrothermal ZnO thin films", *Journal of Electronic Materials*, **46**(3), pp. 1821-1825 (2017).
28. Ghasaban, S., Atai, M., Imani, M., et al. "Facile templateless fabrication of ZnO nanostructures: A consideration of several parameters", *Scientia Iranica, Transactions F, Nanotechnology*, **23**(6), p. 3163 (2016).
29. Singh, S., Gupta, D., Jain, V., et al. "Microwave processing of materials and applications in manufacturing industries: A review", *Materials and Manufacturing Processes*, **30**(1), pp. 1-29 (2015).
30. Nguyen, N.T., Nguyen, B.H., Ba, D.T., et al. "Microwave-assisted synthesis of silver nanoparticles using Chitosan: A novel approach", *Materials and Manufacturing Processes*, **29**(4), pp. 418-421 (2014).
31. Wang, Z., Sun, P., Yang, T., et al. "Flower-like WO_3 architectures synthesized via a microwave-assisted method and their gas sensing properties", *Sensors and Actuators B: Chemical*, **186**, pp. 734-740 (2013).
32. Charles, J., Lawrence, N., and Thiruvenkadam, S. "Structural and optical properties of nanostructured zinc oxide thin films by spray pyrolysis and ethanol sensing", *Physics Procedia*, **49**, pp. 92-99 (2013).
33. Zhu, L. and Zeng, W. "Room-temperature gas sensing of ZnO-based gas sensor: A review", *Sensors and Actuators A: Physical*, **267**, pp. 242-261 (2017).
34. Kiani, G., Nourizad, A., and Nosrati, R. "In-situ chemical synthesis of polypyrrole/silver nanocomposite for the use as a room temperature ammonia gas sensor", *Fibers and Polymers*, **19**(10), pp. 2188-2194 (2018).
35. Trinh, T.T., Tu, N.H., Le, H.H., et al. "Improving the ethanol sensing of ZnO nano-particle thin films-the correlation between the grain size and the sensing mechanism", *Sensors and Actuators B: Chemical*, **152**(1), pp. 73-81 (2011).
36. Wang, Q., Kou, X., Liu, C., et al. "Hydrothermal synthesis of hierarchical CoO/SnO_2 nanostructures for ethanol gas sensor", *Journal of Colloid and Interface Science*, **513**, pp. 760-766 (2018).

Biographies

Gholamreza Kiani holds a PhD in Chemistry and is currently Associate Professor in the School of Engineering, Emerging Technologies, at University of Tabriz. His research interests include gas, thermal, and IR sensors.

Abolfazl Nourizad is PhD candidate in Electrical Engineering at University of Tabriz. His research interests are electrical devices, including sensors and conducting polymers.

Rahimeh Nosrati obtained her BS, MSc, and PhD degrees in Applied Chemistry from University of Tabriz. She is currently a Post-Doctoral researcher in the School of Engineering, Emerging Technologies, at University of Tabriz. Her main research interests are conducting polymers, sensors, and coatings.